Ab initio and classical molecular dynamics of neon melting at high pressure

L. Koči,[1] R. Ahuja,[1,2] and A. B. Belonoshko[2,3]
[1]*Condensed Matter Theory Group, Physics Department, Uppsala University, Box 530, SE-751 21 Uppsala, Sweden*
[2]*Applied Materials Physics, Department of Materials Science and Engineering, The Royal Institute of Technology, SE-100 44 Stockholm, Sweden*
[3]*Condensed Matter Theory, Alba Nova University Center, Physics Department, The Royal Institute of Technology, SE-106 91 Stockholm, Sweden*
(Received 25 January 2007; published 15 June 2007)

First-principles and classical molecular dynamics calculations have been performed to study the high-pressure melting curve of Ne. In the low temperature region, simulations with solid and liquid in coexistence (two-phase) with a Lennard-Jones interatomic potential well reproduce experimental findings. As anticipated, there is a melting temperature overestimation when heating a crystal (one-phase) compared to the two-phase results. Furthermore, there is a significant discrepancy comparing the one-phase *ab initio* curve to previously reported classical predictions: at 150 GPa, the calculations in this work show a melting temperature approximately 1000 K above the estimate based on an exponential-6 potential. However, there is a close match between the one-phase *ab initio* curve and the classical one-phase results in this work. This could also imply an agreement between a two-phase *ab initio* and classical two-phase melting curve. Therefore, considering the documented accuracy of the coexistence method, the classical two-phase melting in this work could well indicate the most probable melting behavior. In conjunction with recent theoretical results for Xe, no significant melting slope decrease was observed for Ne in this study.

DOI: 10.1103/PhysRevB.75.214108 PACS number(s): 64.70.Dv

I. INTRODUCTION

Noble gases such as He, Ne, Ar, Kr, and Xe have filled electron shells making them stable and unreactive. Their stability makes experimental studies relatively simple. Therefore, the comparison of experimental and theoretical studies of the noble gases are benefited from these ideal systems. Studies of noble gases under high pressure are of fundamental interest as they can be used as a pressure medium in the diamond-anvil cell (DAC) measurements.[1,2] Furthermore, for planetological purposes, noble gas geochemistry can serve as a tool for obtaining information on the early history and composition of the Earth.

The metalization of Ne is very different compared to the heavier gases Ar, Kr, and Xe as the energy band gap between the valence $2p$ states and the unoccupied $3d$ states is large. For argon, krypton, and xenon however, the p states are very well hybridized with the corresponding d states. This discrepancy makes the neon melting highly interesting at extreme conditions.

For Ne, a number of high-pressure experiments have been performed using the DAC technique[3–5] and piston-displacement methods.[6] During the last 15 years, the experimental methods of compressing noble and diatomic gases have developed from a low pressure range to very high pressure. From this advancement, the experimental database in the multimegabar pressure domain is expected to grow, also resulting in the improvement of simple-molecular system theories.

Due to the van der Waals forces which are dominating the bonding character of closed-shell systems, the theoretical models using two-body interatomic potentials can fairly well describe the properties of the Ne gas.[3]

Neon crystallizes into a face-centered-cubic (fcc) structure at 24.4 K and ambient pressure.[7] X-ray diffraction studies at room temperature by Hemley *et al.*[5] show no solid-solid phase transitions up to 110 GPa. Furthermore, a possible fcc-bcc (body-centered-cubic) transition at high temperature should not affect the melting temperature significantly.[8] Therefore, in this work, only the fcc phase has been considered in the applied pressure (P) and temperature (T) range.

An important aspect of performing theoretical calculations is an extended knowledge of material properties in a PT domain not yet reached in experiments. In this study, classical as well as first-principles (*ab initio*) calculations, based on the density-functional theory (DFT),[9] have been performed. Calculations based on empirical potentials are fast compared to first-principles methods which require extensive computer time. Therefore, the former can serve as an indication for the PT melting conditions before performing the *ab initio* calculations. To the authors' knowledge, the high-pressure and high-temperature melting curve of Ne has not been studied previously by first-principles methods. Although DFT does not accurately describe the van der Waals bonding, the method is still valid as the strong repulsion at short interatomic distances is dominant at high pressures.[10]

Although extensive theoretical studies of melting have been performed during the last few decades, there are still uncertainties regarding this structural transition.[11] Melting can be divided into two subcategories: homogeneous, where the melting initiates in the bulk region, resulting in atomic displacements from the lattice positions, and heterogeneous, where the atoms diffuse at the surfaces.[12] By using any typical molecular dynamics (MD) code, temperature can be applied to a crystal at constant volume or pressure. If periodic boundary conditions (PBC) are used, the surface effects are absent. Therefore, a temperature high enough to force atomic displacements implies homogeneous melting. However, the

overheating to find the melting point can be substantial compared to the true melting temperature, T_m. The limit of superheating, T_{LS}, can overshoot T_m by as much as 30%.[13] By studying one-phase and two-phase simulations, the difference between the melting temperatures can be estimated.

One of the motivations of the present work is to compare the melting of Ne to experimental results of heavier rare gas elements Ar, Kr, and Xe where an anomalous change of the melting slope, later assigned to be a solid-solid transition,[14] was observed.[4] Furthermore, as the *p-d* gap for Ne is large compared to Ar, Kr, and Xe, another purpose of performing *ab initio* calculations is to see the effect of electronic structure on melting. In this paper we first describe the classical and DFT methods used. The results are followed by a discussion and a conclusion.

A. The models

The development of first-principles (*ab initio*) methods have been reported in numerous papers and books,[15–19] and the ongoing progress of electronic structure calculations is highly important in several scientific fields. The improvement of numerical algorithms in combination with an increasing performance of computer systems continue to cut simulation times. However, *ab initio* simulations are still limited to operate only on relatively small systems.[20] Representing the other extreme of the spectra, classical MD is relatively fast. As the electronic effects are incorporated in the interatomic potentials, and thus no electrons are treated explicitly in the calculations, the simulations can treat millions of atoms.

Although having a simple two-body form, the exponential-6 (Exp-6) potential used in this work has been successfully applied to noble gases.[3,21–24] The potential is defined as

$$\Phi(r) = \epsilon\left[\frac{6}{\alpha-6}e^{\alpha(1-r/r_m)} - \frac{\alpha}{\alpha-6}\left(\frac{r_m}{r}\right)^6\right], \qquad (1)$$

where ϵ is the depth of the interatomic well, α controls the stiffness at small interatomic distances, and r_m is the well minimum position. The parameters are $\epsilon/k=42.0$ K, $r_m=3.18$ Å, and $\alpha=13.2$, as reported by Vos *et al.*[3] The parameters were found by fitting to piston cylinder experiments at 2 GPa and to two DAC experiments conducted at 15 and 110 GPa, respectively. Hemley *et al.*[5] present similar parameters, emphasizing their validity to reproduce Ne properties at high pressures.

Furthermore, the Lennard-Jones (LJ) potential

$$\Phi(r) = 4\epsilon\left[\left(\frac{\sigma}{r}\right)^{12} - \left(\frac{\sigma}{r}\right)^6\right], \qquad (2)$$

has shown to reproduce thermodynamic properties of gases such as argon,[25,26] xenon,[27] and krypton.[28] In this work, we have examined the potential parameters for neon with $\epsilon/k=35.1$ K (k is the Boltzmann constant) and $\sigma=2.72$ Å from Bellissent-Funel *et al.*[29] and $\epsilon/k=52.2$ K; $\sigma=2.70$ Å from Acocella *et al.*[30] The two LJ potentials together with the Exp-6 interaction are shown in Fig. 1.

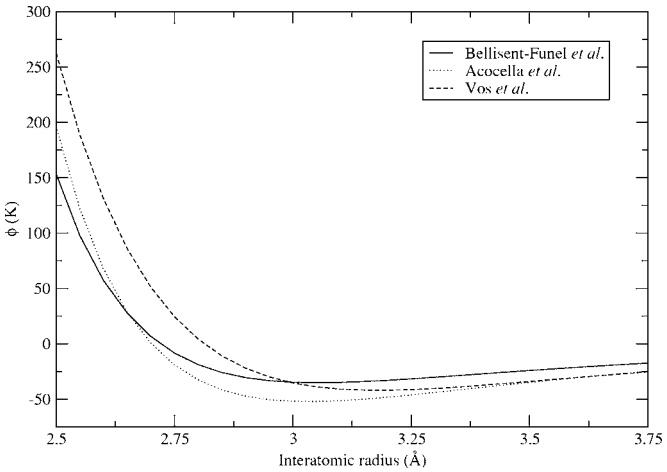

FIG. 1. Comparison of the interatomic potential for Ne from Bellissent-Funel *et al.* (Ref. 29), Acocella *et al.* (Ref. 30), and Vos *et al.* (Ref. 3).

B. Technical details

1. Classical MD

The MOLDY package[31] was used for the calculations, where the complete description of the methods used in the code can be found in the manual. The simulations were performed in the *NPT* (constant number of particles together with constant pressure and temperature) ensemble, using a Nosé-Hoover thermostat for the temperature control and a Parrinello and Rahman method for the pressure.[31] Periodic boundary conditions were applied, meaning that if a particle leaves the simulation box, an identical particle enters on the other side. The time step was set to $dt=0.5$ fs and the cutoff radius to $r=6$ Å. A strict cutoff was applied, meaning that all interactions between pairs of sites within the cutoff were included.

2. Ab initio calculations

The DFT calculations in this work were performed in a *NVT* ensemble (constant number of particles, constant volume and temperature) using the Vienna *Ab Initio* Simulation Package (VASP).[32,33] Ultrasoft pseudopotentials were used to represent the ionic cores. For the comparison of the calculations, two exchange-correlation functions were used, namely the local-density approximation (LDA) and the generalized-gradient approximation (GGA).[34] An adequate energy convergence was reached with a $4\times4\times4$ Monkhorst-Pack **k**-point grid and the cutoff energy was 450 eV. When performing the *ab initio* molecular dynamics (AIMD), the size of the time step was 0.5 fs. In conjunction with other recent studies, only the Γ point was used for the Brillouin zone integrations to avoid too long simulation times.[35,36]

II. RESULTS

To generate crystals for the calculations, perfect fcc lattices containing 864 and 108 atoms were constructed. The four-atom fcc unit cell was multiplied 6 times (3 times) in the three orthogonal directions x, y, and z ($4\times6\times6\times6$ and

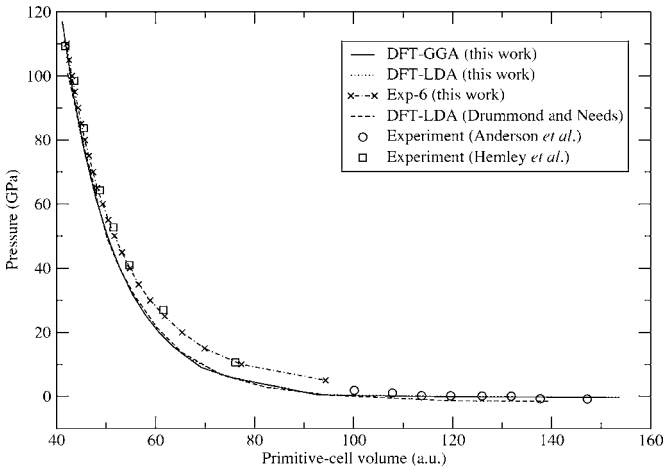

FIG. 2. Equation of state (EOS) with pressure as a function of volume. The *ab initio* results using the exchange-correlation functions LDA and GGA from this work are almost coinciding, whereas the classical MD simulations at 293 K perfectly match experimental data. The results are compared to theory [Drummond and Needs (Ref. 10)] and experiment [Hemley *et al.* (Ref. 5) and Anderson *et al.* (Ref. 6)].

$4\times3\times3\times3$, respectively). The initial lattice parameters were varied from $a=2.90$ to 3.90 Å to represent the approximate densities in the studied pressure and temperature range. To calculate the equation of state (EOS), the third-order Birch-Murnaghan (BM) was used.[37,38] The energy $E(x)$ and pressure $P(x)$ are defined as

$$E(x) = E_0 + \frac{3}{2}B_0V_0 \times\left(\frac{3}{2}(\chi-1)x^{2/3} + \frac{3}{4}(1-2\chi)x^{4/3} + \frac{1}{2}\chi x^{6/3} - \frac{2\chi-3}{4}\right) \tag{3}$$

and

$$P(x) = \frac{3}{2}B_0[x^{7/3}-x^{5/3}](1+\chi[x^{2/3}-1]), \tag{4}$$

where V_0 is the zero-pressure volume, B_0 and B_0' is the bulk modulus and pressure derivative of the bulk modulus, $x=V_0/V$ and $\chi=\frac{3}{4}(B_0'-4)$. Drummond and Needs[10] have reported indistinguishable pressure-volume data when comparing the Vinet and BM EOS at high compression. Thus, without any further investigation regarding the most suitable EOS, the BM equations were used throughout this study. The EOS showing pressure as a function of primitive-cell volume is shown in Fig. 2. Comparing the exchange correlations LDA with GGA shows similar results. However, for the coming calculations, the LDA was chosen as it has been reported to perform better when calculating the ground-state properties of another noble gas, Xe.[21] The classical simulations, using the Exp-6 potential in the *NPT* ensemble with $T=293$ K, show a perfect agreement with the experimental results from Hemley *et al.*[5] To initiate the setup for the two-phase simulations, two perfect fcc lattices containing 864 atoms each were constructed, as previously described. One of these lattices, shown as (1) in Fig. 3, was simulated at a high temperature to transform into a molten configuration. The solid and molten structures were put together with a small spacing in a simulation box, letting the lower part of the box be solid and the upper part be liquid, as shown in (2) in Fig. 3. Starting from this configuration, the MD simulations result in a monophase. If the temperature is above the melting temperature T_m, the phase will become liquid (3a) whereas the phase will solidify if the temperature is below T_m (3b). By narrowing the interval, the melting temperature can be estimated at the specific pressure in the simulation. Belonoshko[20] and Tepper and Briels[39] explain the two-phase simulation method in detail, and its successful application for a number of systems has been reported.[18,40–42] For the rare gases in particular, the technique has recently been employed to study the melting of Xe.[14] An effective way of describing the average structure of disordered molecular systems is the evaluation of the radial distribution function (RDF). The function can be deduced experimentally from x-ray or neutron diffraction studies, thus providing a direct comparison between experiment and simulation. As a tool to find the melting properties from simulations near solid-fluid phase boundaries, the RDF has been widely used in MD.[21,43–46]

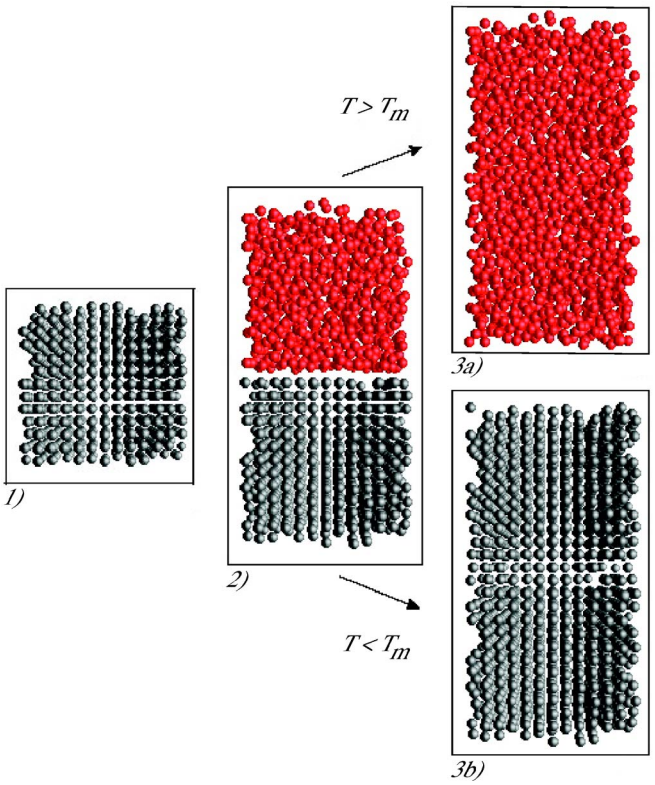

FIG. 3. (Color online) 864 atoms in a fcc structure are shown in (1). By melting an identical lattice, a two-phase setup can be constructed, as shown in (2). Here, the 864 atoms in the molten structure are placed on top of the 864 atoms in the fcc structure. Starting from this configuration, the MD simulations result in a monophase. If $T>T_m$, the phase will become liquid (3a) whereas the phase will solidify if $T<T_m$ (3b). By narrowing the interval, the melting temperature can be estimated at the specific pressure in the simulation.

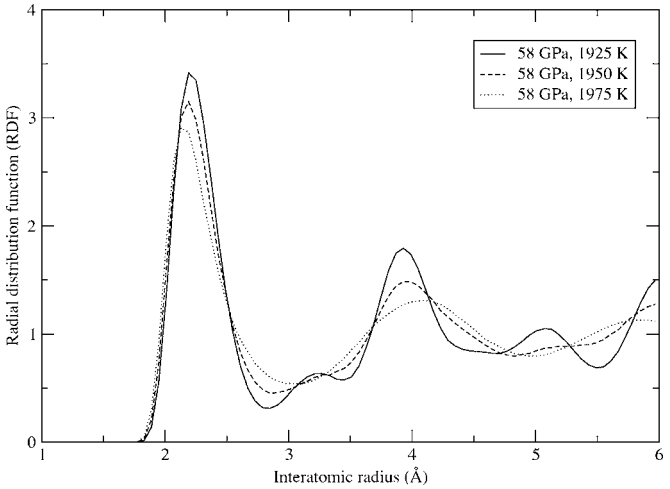

FIG. 4. The radial distribution function (RDF) from simulations with the Lennard-Jones (LJ) potential from Bellissent-Funel *et al.* performed at $P=58$ GPa and $T=1925$, 1950, and 1975 K, respectively. At $T=1925$ K, the RDF shows distinct peaks, indicating a solid structure. At $T=1950$ K the configuration tends to liquefy. At $T=1975$ K, the smooth curve of the RDF emphasizes a liquid structure.

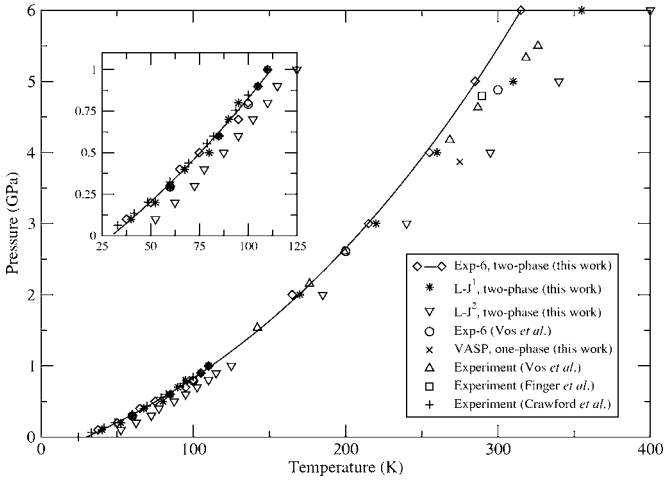

FIG. 5. The melting curve of neon in the low temperature region. The theoretical predictions from this work were performed with the two-phase setup shown as (2) in Fig. 3. The atomic interactions used were the Exp-6 potential from Vos *et al.* (Ref. 3) and the Lennard-Jones potential from Bellissent-Funel *et al.* (Ref. 29) (denoted as LJ^1) and Acocella *et al.* (Ref. 30) (denoted as LJ^2), respectively. As the latter potential shows a stiffer repulsion in Fig. 1, a higher temperature is required at a specific pressure, compared to the Exp-6 and the LJ by Bellissent-Funel *et al.* The *ab initio* melting point, found from the one-phase calculations, show a small $(\sim 5\%)$ melting temperature overshoot compared to experiment.

The distribution function $g_n(r)$ can be defined in the following way: over an interval of n time steps of integration of the equations of motion, the mean volume V_n and the mean number of atoms N_n, at a distance between r and $r+dr$ from an atom, are calculated. Then, $g_n(r)$ is given by

$$g_n(r) = \frac{N_n(r)V_n}{4\pi r^2 dr N}. \tag{5}$$

Figure 4 demonstrates the possibility to detect melting by means of the $g_n(r)$. Shown in the figure are the distribution functions from the two-phase simulations with the Lennard-Jones potential from Bellissent-Funel *et al.*[29] performed at $P=58$ GPa and $T=1925$, 1950, and 1975 K, respectively. As the temperature in the respective simulations is increased, the distinct peaks, indicating a solid structure at $T=1925$ K, start to vanish. Instead, the $g_n(r)$ shows a lower first peak and a smoother curve at $T=1975$ K, indicating a liquid structure.

In Fig. 5, the melting pressure as a function of temperature is shown. Due to the stiff parameter setting from Acocella *et al.*,[30] the melting curve does not follow experimental data.[3,47,48] For pressures up to 1 GPa, the results from the parameter settings from Bellissent-Funel *et al.*[29] and Vos *et al.*[3] are almost overlapping and compare well to experimental data.[48] However, at higher pressures, the LJ potential[29] shows a better agreement with experiment. When calculating the $g_n(r)$ for small atomic systems, the function can show a more noisy behavior as compared to bigger systems.[49] As a result, a melting determination can become more difficult and imprecise. Therefore, diffusion analysis can serve as a complementary criterion. By increasing the temperature in the one-phase AIMD calculations, the solid structure melts, indicated by the atomic movements as shown in Fig. 6. Each small circle represents the x and y atomic coordinates in the MD simulation box, where the choice of a two-dimensional presentation is due to enhanced visualization. A small circle is shown every 50th time step. For the leftmost image, the circles appear in the vicinity of each atomic site, as the structure shows solidlike behavior. By increasing the temperature from 700 to 900 K, the atoms start to diffuse. This can be seen as the atoms tend to leave their positions in the solid configuration to spread in the simulation box, shown in the middle and rightmost image. As a complement to the visual determination of the melting in Fig. 6, the mean square displacement (MSD) was calculated. For a species of N particles, the MSD is calculated as

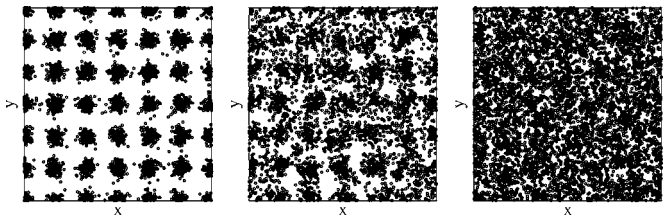

FIG. 6. Atomic displacement as a function of time and space. Each small circle represents the x and y coordinates for the atoms in the simulation box, where the two-dimensional presentation is due to enhanced visualization. A circle is shown every 50th time step. From left to right, the temperature is 700, 800, and 900 K, respectively. In the leftmost image, the atoms are relatively fixed in their positions whereas the atoms start to leave their atomic sites to diffuse, as shown in the middle and rightmost image.

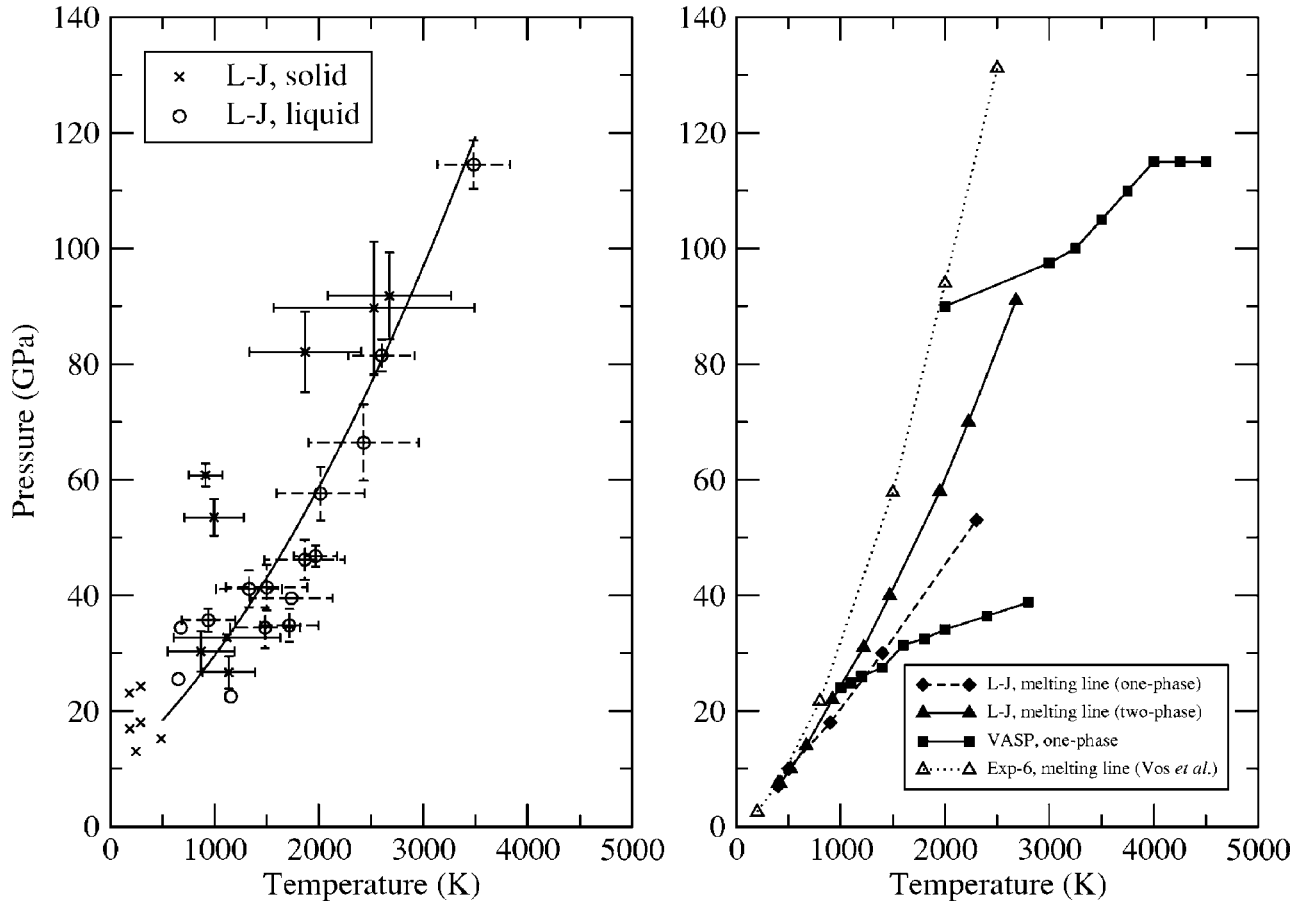

FIG. 7. The estimated melting of Ne in a high pressure region comparing different methods. To resemble the limits of the *ab initio* calculations, small configurations (108+108 atoms) with the same LJ potential in a canonical ensemble were simulated for short times (3000 time steps), shown in the left-hand figure. To distinguish a solid phase (stars) from a liquid phase (circles) the $g_n(r)$ was applied, using the last couple of 100 time steps. From this ensemble, the pressure and temperature uncertainty was calculated in the MD program, expressed as error bars in the figure. For some points, small error bars were neglected for enhanced readability. Furthermore, as a guide for the eye, a curve was inserted for the approximate separation of the solid and liquid regime. In the right-hand figure, the melt line for the 1728 atom system (864+864, two phase) with the LJ interaction from Bellissent-Funel *et al.* (Ref. 29) was found by means of the $g_n(r)$. The simulations were performed for 40 000 time steps. Furthermore, the melt line from one-phase 108 atom simulations over 3000 time steps with the same potential is shown. At approximately 30 and 100 GPa, the *ab initio* MD calculations showed discontinuities in the *PT* diagram, indicating melting. Compared to the big two-phase system, the temperature overshoot is approximately 300 and 500 K, respectively, which is quite reasonable. The melting curve from Vos *et al.* (Ref. 3) is also inserted.

$$\langle |\mathbf{r}(t) - \mathbf{r}(0)|^2 \rangle = \frac{1}{NN_t} \sum_{n=1}^{N} \sum_{t_0}^{N_t} |\mathbf{r}_n(t+t_0) - \mathbf{r}(t_0)|^2, \qquad (6)$$

where $\mathbf{r}(t)$ is the atomic position at time t and $\mathbf{r}(0)$ is the initial atomic position. The diffusion parameter D, which is proportional to the slope of the mean square displacement at long times, is calculated using the Einstein relation

$$\langle |\mathbf{r}(t) - \mathbf{r}(0)|^2 \rangle = 6Dt. \qquad (7)$$

The diffusion parameter was analyzed as a function of temperature at constant volume in the calculations. A steep increase of D was seen at the temperatures where the atoms started to show a distinctively enhanced diffusion as shown in Fig. 6.

To resemble the limits of the *ab initio* calculations, small two-phase configurations (108+108 atoms) with the same LJ potential in a canonical ensemble were simulated for short times (3000 time steps), shown to the left in Fig. 7. The $g_n(r)$ was used to distinguish a solid phase (stars) from a liquid phase (circles). The small and short *NVT* two-phase calculations follow the big and long *NPT* simulations well, shown to the right in Fig. 7. The melt lines for the 1728 atom system (864+864, two-phase) and the 108 atom configuration (one-phase) with the LJ interaction from Bellissent-Funel *et al.*[29] were found by means of the radial distribution function. The simulations were performed for 40 000 and 3000 time steps, respectively. There is a discrepancy between the small and short one-phase runs and the big and long two-phase runs, as the former tend to overshoot the melting temperature. According to previous studies,[13,50] this is expected.

At approximately 30 and 100 GPa, the AIMD calculations with 108 atoms show discontinuities for the pressures in Fig. 7 at melting. This is related to the rise in kinetic energy with atomic movement, rapidly increasing the pressure. The melt-

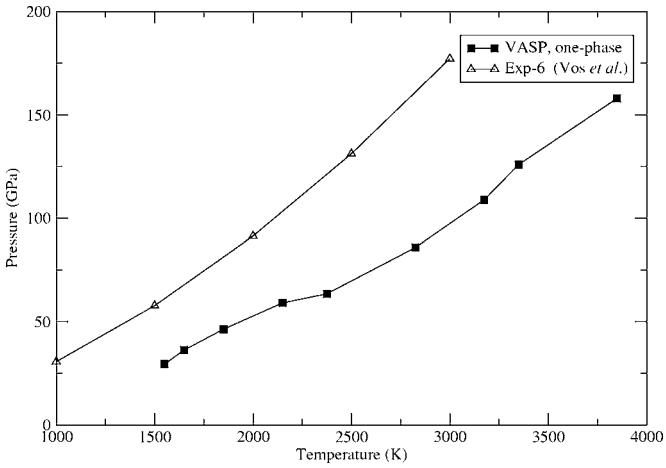

FIG. 8. The high pressure melting curve of Ne from this work compared to the predicted melting from Vos *et al.* (Ref. 3). The melting points in this study were found from visual inspection of the atomic diffusion and the MSD in Eq. (6).

ing was also confirmed by visual inspection of the diffusion, as shown in Fig. 6. Compared to the results from the big two-phase system, the melting temperature overshoot from the *ab initio* calculations shown in the figure is approximately 300 and 500 K, respectively, which is quite reasonable. The classical and *ab initio* melting results from this work are compared with one of the few predicted melting curves of neon at extreme conditions from Vos *et al.*[3] The discrepancy at high pressure and high temperature between this prediction and the classical coexistence results in this work could be explained by two observations. Vos *et al.* calculate the free energy for the liquid and solid, respectively, and find the melting at the intersection points. In this study, a two-phase approach is applied and the melting is analyzed with the $g(r)$. More importantly, however, is the use of different interatomic potentials.

Figure 8 shows the AIMD melting curve estimate, based on diffusion analysis, from an initial 108-atom fcc crystal. The predicted melting from Vos *et al.*[3] is also inserted. Clearly, there is a big discrepancy, as the AIMD one-phase calculations need significantly higher temperatures to melt the crystal. However, this melting follows the one-phase LJ curve shown in Fig. 7 quite accurately. This could also indicate the conformity between the *ab initio* and classical two-phase calculations, where the melting accuracy of the previous method has been reported.[40–42] Therefore, the *ab initio* one-phase melting from this work and the Vos *et al.* melting curve might well serve as higher and lower bounds for the most probable melting behavior.

Vos *et al.* report that changing the parameter setting in Eq. (1) from $\alpha=14.66$ (Ref. 51) to $\alpha=13.2$ gives a better fit for the solid and liquid volumes at high pressures. Based on these studies, however, the melting curve by Vos *et al.* is low compared to the findings in this work. Even though one-phase simulations in MD might overestimate the true melting temperature, it is highly unlikely that *ab initio* two-phase calculations would reveal a melting curve in such a low temperature regime.

For the heavier noble gases Xe, Kr, and Ar, DAC studies from Boehler *et al.*[4] have shown good agreement with the scaled neon melting curve.[3] However, at approximately 20, 30, and 40 GPa, respectively, a distinct lowering of the experimental melting temperatures occurs. The kink is rather smooth for Ar, but becomes sharper for Kr and Xe. As impurities lead to a melting temperature decrease compared to pure crystals,[52] Boehler *et al.* suggested stacking faults in the fcc structure. The faults could occur from thermal fluctuations, constructing hexagonal close-packed (hcp) microstructures. This theory was later abandoned by the authors,[53] referring to the full hcp structure above 41 GPa for Xe.[54] Instead, the pressure induced p to d hybridization, which could favor liquid structures with icosahedral short-range order[55] was considered as an explanation. However, recent AIMD results from Belonoshko *et al.*[14] do not indicate any anomalous melting behavior of Xe, although the calculations take the p to d hybridization into account. Instead, the authors explain the experimental findings as a solid-solid temperature induced phase transformation. For the melting of Ne in Fig. 8, no significant kink is seen which could indicate a melting temperature decrease at high pressure.

III. DISCUSSION AND CONCLUSION

Melting is a complex transition, still under intensive investigation. In the high-pressure and high-temperature range, experimental results on noble gas melting are still scarce, making the feedback to the theoretical models more difficult. To achieve a more accurate description of melting curves, it is important to analyze a combination of melting criteria based on, e.g., diffusivity, distributions or other thermodynamic methods. Furthermore, the limits of the systems and calculations, both for classical and *ab initio* approaches, must be taken into account. In accordance with other *ab initio* studies,[35,36] the system in this study has been limited to 108 atoms in a one-phase configuration. Ahuja *et al.*[50] report the risk of overheating in one-phase simulations in MD to find the melting temperature. However, performing bigger two-phase AIMD calculations, where liquid and solid configurations are simulated together, are extremely time consuming. Delogu[12] reports an increasing homogeneous melting point for fcc-Al in the order of 10% when increasing the system from 864 to 6912 atoms. This implies that the system size could influence the results of this study.

In this paper, we have investigated the melting at high pressure of Ne using classical and *ab initio* methods. The melting conditions determined from the mean square displacements and the atomic diffusion from visual inspection have been found to be mutually consistent. By comparing classical one- and two-phase MD calculations, we have shown that the melting temperatures found by the one-phase configurations are slightly overestimated due to overheating. Although the high-pressure Ne melting curve determined by AIMD one-phase simulations is high compared to classical predictions,[3] it is found close to the classical one-phase results. Therefore, considering the documented accuracy of the two-phase method, the true melting curve could be found closer to the classical two-phase results from this work rather than to the Exp-6 potential findings previously reported.

Although taking pressure-induced electronic changes into account, recent theoretical results[14] do not show any satura-

tion of the Xe melting curve, previously reported by experiment.[4] Our study also shows that the melting of Ne looks similar to the theoretical melting curves of Ar, Kr, and Xe. This implies that *p-d* hybridization should not be responsible for any anomalous behavior as suggested experimentally for the heavier gases.

ACKNOWLEDGMENTS

One of the authors (L.K.) wishes to thank K. Refson for the MD simulation package. This work was supported by the Swedish Research Council (VR) and the European Science Foundation (ESF) in the framework of the EuroMinSci project.

[1] P. M. Bell and H. K. Mao, Year Book - Carnegie Inst. Washington **80**, 404 (1981).
[2] K. Takemura, J. Appl. Phys. **89**, 662 (2001).
[3] W. L. Vos, J. A. Schouten, D. A. Young, and M. Ross, J. Chem. Phys. **94**, 3835 (1990).
[4] R. Boehler, M. Ross, P. Söderlind, and D. B. Boercker, Phys. Rev. Lett. **86**, 5731 (2001).
[5] R. J. Hemley, C. S. Zha, A. P. Jephcoat, H. K. Mao, L. W. Finger, and D. E. Cox, Phys. Rev. B **39**, 11820 (1989).
[6] M. S. Anderson, R. Q. Fugate, and C. A. Swenson, J. Low Temp. Phys. **10**, 345 (1973).
[7] M. P. Fang and P. E. Sokol, Phys. Rev. B **52**, 12614 (1995).
[8] A. B. Belonoshko, R. Ahuja, and B. Johansson, Phys. Rev. Lett. **87**, 165505 (2001).
[9] P. Hohenberg and W. Kohn, Phys. Rev. **136**, 864 (1964).
[10] N. D. Drummond and R. J. Needs, Phys. Rev. B **73**, 024107 (2006).
[11] R. W. Cahn, Nature (London) **413**, 582 (2001).
[12] F. Delogu, J. Phys.: Condens. Matter **18**, 5639 (2006).
[13] A. B. Belonoshko, N. V. Skorodumova, A. Rosengren, and B. Johansson, Phys. Rev. B **73**, 012201 (2006).
[14] A. B. Belonoshko, S. Davis, A. Rosengren, R. Ahuja, B. Johansson, S. I. Simak, L. Burakovsky, and D. L. Preston, Phys. Rev. B **74**, 054114 (2006).
[15] I. H. F. Schaefer, *Properties of Complex Inorganic Solids* (Dover, New York, 2004).
[16] L. Stixrude, R. E. Cohen, and D. J. Singh, Phys. Rev. B **50**, 6442 (1994).
[17] P. Söderlind, J. A. Moriarty, and J. M. Wills, Phys. Rev. B **53**, 14063 (1996).
[18] A. B. Belonoshko, R. Ahuja, and B. Johansson, Phys. Rev. Lett. **84**, 3638 (2000).
[19] A. P. Jardine, S. Dworski, P. Fouquet, G. Alexandrowicz, D. J. Riley, G. Y. H. Lee, J. Ellis, and W. Allison, Science **304**, 1790 (2004).
[20] A. B. Belonoshko, Geochim. Cosmochim. Acta **58**, 4039 (1994).
[21] A. B. Belonoshko, O. LeBacq, R. Ahuja, and B. Johansson, J. Chem. Phys. **117**, 7233 (2002).
[22] F. Saija and S. Prestipino, Phys. Rev. B **72**, 024113 (2005).
[23] H. T. Lotz and J. A. Schouten, Phys. Rev. B **64**, 024103 (2001).
[24] L. Koči, R. Ahuja, A. B. Belonoshko, and B. Johansson, J. Phys.: Condens. Matter **19**, 016206 (2007).
[25] J. A. Barker and D. Henderson, Rev. Mod. Phys. **48**, 587 (1976).
[26] B. E. Clements, C. E. Campbell, P. J. Samsel, and F. J. Pinski, Phys. Rev. A **44**, 1139 (1991).
[27] E. E. Polymeropoulos, P. Bopp, J. Brickmann, L. Jansen, and R. Block, Phys. Rev. A **31**, 3565 (1985).
[28] J. M. Houlrik, D. P. Landau, and S. J. Knak Jensen, Phys. Rev. E **50**, 2007 (1994).
[29] M. C. Bellissent-Funel, U. Buontempo, A. Filabozzi, C. Petrillo, and F. P. Ricci, Phys. Rev. B **45**, 4605 (1992).
[30] D. Acocella, G. K. Horton, and E. R. Cowley, Phys. Rev. B **61**, 8753 (2000).
[31] K. Refson, Moldy User's Manual, release 2.16 (2001).
[32] G. Kresse and J. Hafner, Phys. Rev. B **47**, 558 (1993).
[33] G. Kresse and J. Furthmüller, Phys. Rev. B **54**, 11169 (1996).
[34] J. P. Perdew, K. Burke, and M. Ernzerhof, Phys. Rev. Lett. **77**, 3865 (1996).
[35] P. A. Fedders, Phys. Rev. B **64**, 165206 (2001).
[36] H. W. Sheng, W. K. Luo, F. M. Alamgir, J. M. Bai, and E. Ma, Nature (London) **439**, 419 (2006).
[37] F. Birch, Phys. Rev. **71**, 809 (1947).
[38] F. Birch, J. Geophys. Res. **83**, 1257 (1978).
[39] H. L. Tepper and W. J. Briels, J. Cryst. Growth **230**, 270 (2001).
[40] A. B. Belonoshko, R. Ahuja, O. Eriksson, and B. Johansson, Phys. Rev. B **61**, 3838 (2000).
[41] D. Alfè, M. J. Gillan, and G. D. Price, J. Chem. Phys. **116**, 6170 (2002).
[42] A. Laio, S. Bernard, G. L. Chiarotti, S. Scandolo, and E. Tosatti, Science **287**, 1027 (2000).
[43] S. Kambayashi and J. Chihara, Phys. Rev. E **53**, 6253 (1996).
[44] A. B. Belonoshko, R. Ahuja, and B. Johansson, Phys. Rev. B **61**, 11928 (2000).
[45] R. Boehler, M. Ross, and D. B. Boercker, Phys. Rev. Lett. **78**, 4589 (1997).
[46] L. Koči, A. B. Belonoshko, and R. Ahuja, Phys. Rev. B **73**, 224113 (2006).
[47] L. W. Finger, R. M. Hazen, G. Zou, H. K. Mao, and P. M. Bell, Appl. Phys. Lett. **39**, 892 (1981).
[48] R. K. Crawford and W. B. Daniels, J. Chem. Phys. **55**, 5651 (1971).
[49] P. Ganster, M. Benoit, W. Kob, and J. M. Delaye, J. Chem. Phys. **120**, 10172 (2004).
[50] R. Ahuja, A. B. Belonoshko, and B. Johansson, Phys. Rev. E **57**, 1673 (1998).
[51] P. J. Koortbeek and J. A. Schouten, Mol. Phys. **69**, 981 (1990).
[52] P. C. Liu, P. R. Okamoto, N. J. Zaluzec, and M. Meshii, Phys. Rev. B **60**, 800 (1999).
[53] M. Ross, R. Boehler, and P. Söderlind, Phys. Rev. Lett. **95**, 257801 (2005).
[54] H. Cynn, C. S. Yoo, B. Baer, V. Iota-Herbei, A. K. McMahan, M. Nicol, and S. Carlson, Phys. Rev. Lett. **86**, 4552 (2001).
[55] A. L. McKay, Acta Crystallogr. **15**, 916 (1962).